HiLumi LHC

FP7 High Luminosity Large Hadron Collider Design Study

Scientific / Technical Note

"How to maximize the HL-LHC performance (HL-LHC)?"

Arduini, G (CERN) *et al*

29 October 2013

This work is part of HiLumi LHC Work Package **2: Accelerator Physics & Performance**.

HOW TO MAXIMIZE THE HL-LHC PERFORMANCE*

G. Arduini, D. Banfi, J. Barranco, H. Bartosik, R. Bruce, O. Brüning, R. Calaga, F. Cerutti,
H. Damerau, R. De Maria†, L. Esposito, S. Fartoukh, M. Fitterer, R. Garoby, S. Gilardoni,
M. Giovannozzi, B. Goddard, B. Gorini, M. Lamont, E. Métral, N. Mounet, T. Pieloni, S. Redaelli,
L. Rossi, G. Rumolo, E. Todesco, R. Tomas, F. Zimmermann, CERN, Geneva, Switzerland;
A. Valishev, FNAL, Batavia, USA

Abstract

This contribution presents an overview of the parameter space for the HL-LHC [1] upgrade options that would maximize the LHC performance after LS3. The analysis is assuming the baseline HL-LHC upgrade options including among others, 25ns spacing, LIU [2] parameters, large aperture triplet and matching-section magnets, as well as crab cavities. The analysis then focuses on illustrations of the transmission efficiency of the LIU beam parameters from the injection process to stable conditions for physics, the minimization of the luminous region volume while preserving at the same time the separation of multiple vertices, the luminosity control mechanisms to extend the duration of the most efficient data taking conditions together with the associated concerns (machine efficiency, beam instabilities, halo population, cryogenic load, and beam dump frequency) and risks (failure scenarios, and radiation damage). In conclusion the expected integrated luminosity per fill and year is presented.

INTRODUCTION

The Review of the LHC and Injector Upgrade Plans (RLIUP [3]) evaluated the upgrade options for the LHC injectors and the LHC ring. The different upgrades are organized in three scenarios with an increasing number of interventions named PIC [4], US1 [5] and US2 [6] aiming at an integrated luminosity of 1000 fb^{-1}, 2000 fb^{-1}, and 3000 fb^{-1} by 2035, respectively.

The following paper reviews what would be needed to fulfil the US2 goals by analysing the parameter space, by examining the challenges and the hardware interventions foreseen, and by quantifying how close specific scenarios approach the prescribed goal.

PARAMETER SPACE

Under the assumption of 10 years of operation including three long shutdowns and starting with an already accumulated luminosity of 310 fb^{-1} in 2021 [7], the newly upgraded LHC will need to accumulate on average 270 fb^{-1} per year. The integrated performance will be compared by calculating the performance efficiency (η), defined as the fraction of physics time to reach the yearly goal over a period of 160 days, with a sequence of successful fills separated by a 3 h long turnaround (see [8] for a more detailed discussion). Two different fill durations are assumed, a fixed duration of 6 h (the average fill length obtained in 2012 [9]) and the one maximizing the physics efficiency for the respective scenario. For comparison, the 2012 run can be associated with η = 53.5% performance efficiency [8]. Equally suitable definitions of efficiency, which have been used in the review, will not be discussed in this paper since they do not affect the conclusion.

The experiments defined a few experimental conditions that should be fulfilled by the scenarios. For ATLAS and CMS, the average pile-up limit is maximum 140 events per crossing with ideally 0.7 events/mm, but no more than 1.3 events/mm in the luminous region [10]. For LHCb, no more than 4.5 events per crossing can be exploited, while for ALICE the maximum levelled luminosity is assumed to be $2 \cdot 10^{31}$ cm^{-2}s^{-1}[11]. Proton collisions at top energy are assumed to have a total cross section (elastic and inelastic) of 110 mb used for burn-off calculations, while the visible cross section that counts for the observed events is 85 mb for ATLAS and CMS, and 75 mb for LHCb [12-14].

Discussion

While the maximum luminosity tolerated by ATLAS and CMS is widely accepted to be $5 \cdot 10^{34}$ cm^{-2}s^{-1} and an average of 140 event per crossing (HL-LHC baseline), it is interesting to evaluate how this parameter constrains the physics reach. In fact, it is possible to find an upper bound to the performance reach, regardless of the beam conditions by observing that:

$$L_{\text{int}} \leq \ \eta t_{\text{phys}} L_{\text{lev}} \frac{t_{\text{fill}}}{t_{\text{fill}}+ t_{\text{turnaround}}} \quad (1)$$

where L_{int} is the integrated luminosity, t_{phys}, t_{fill}, $t_{\text{turnaround}}$ stand for the physics time, fill duration, and turnaround time, respectively, while L_{lev} is the assumed peak luminosity always levelled without any decay.

Figure 1 shows that the performance goal is theoretically accessible either by increasing the fill time or more effectively by increasing the maximum levelled luminosity. Including the natural decay of the luminosity due to burn-off, the integrated luminosity can be

calculated[‡] by only assuming a value of the virtual luminosity and bunch population at the beginning of the fill [15].

If one assumes the virtual luminosities and starting bunch intensities considered for the HL-LHC project, the picture does not change considerably (Fig. 2) if not excluding the integrated luminosities beyond 300 fb⁻¹ per year for a levelled luminosity of $8 \cdot 10^{34}$ cm⁻²s⁻¹ (see Fig. 2) or barely exceeding 250 fb⁻¹ per year for 10 h fill length.
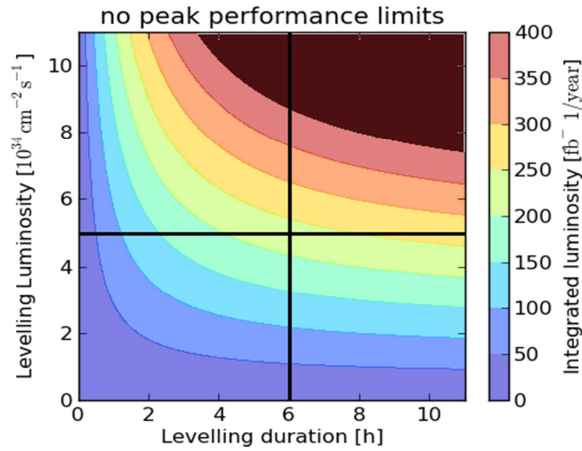

Figure 1: Theoretical LHC performance calculated by assuming 80 days of successful fills (i.e. η = 50 %), 3 h turnaround time and, unrealistically, without any beam related limitations, or equivalently, by assuming that one can always run at the maximum allowed luminosity (see Eq. 1). The black lines highlight the average fill duration of the 2012 LHC run and the baseline maximum instantaneous luminosity tolerated by the ATLAS and CMS experiments. The dark red part represents values above 400 fb⁻¹.

[‡] The equations used are [15]: $\frac{dN}{dt} = -\frac{N}{\tau} = -n_{IP}\sigma L_{lev}$;

$\tau = \frac{N}{n_{IP}\sigma L_{lev}}$; $L_{virt} = k\,L_{lev}$; $t_{lev} = \tau\left(1 - \frac{1}{\sqrt{k}}\right)$; $t_{decay} =$

$\frac{\tau}{2 - \frac{1}{\sqrt{k}}}\left(-1 + \frac{1}{\sqrt{k}} + \sqrt{\left(1 - \frac{1}{\sqrt{k}}\right)^2 + \left(2 - \frac{1}{\sqrt{k}}\right)\frac{t_{turnaround}}{\tau}}\right)$;

$L_{average} = L_{lev}\frac{t_{lev} + \frac{t_{decay}\tau}{t_{decay}+\tau}}{t_{lev}+t_{decay}+t_{turnaround}}$; .
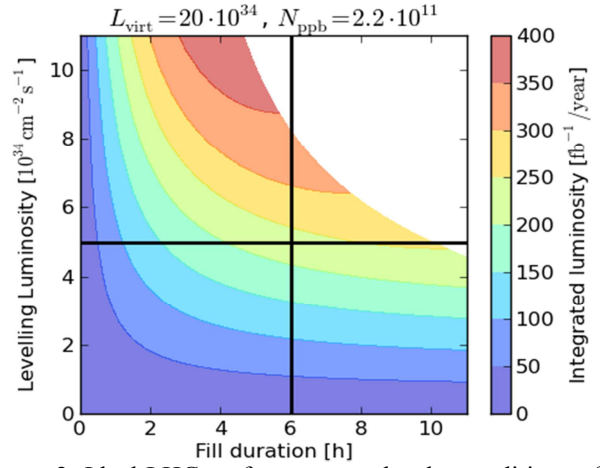

Figure 2: Ideal LHC performance under the conditions of Fig. 1, but including the burn-off decay of the luminosity assuming the peak virtual luminosity and initial bunch population considered for the HL-LHC. The white area is the region for which it would be more efficient to restart a fresh fill and therefore the performance is not evaluated.
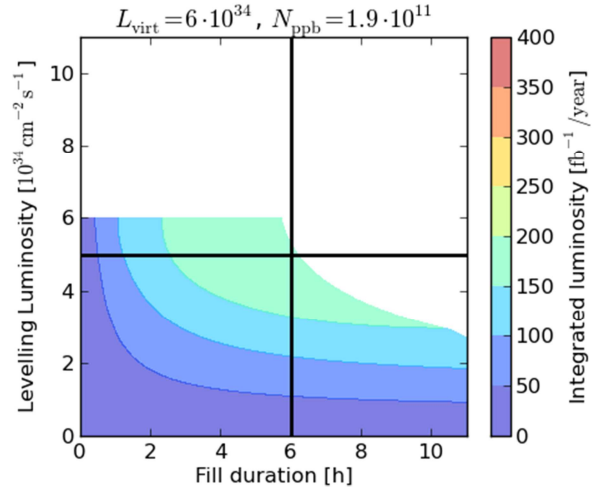

Figure 3: As Fig. 2, but assuming a virtual luminosity much smaller than the ideal scenario (even with large bunch intensity). This scenario does not fully cover the parameter space even under the most conservative assumptions of a levelled luminosity smaller than $5 \cdot 10^{34}$ cm⁻²s⁻¹ and with fill durations smaller than 6 hours.
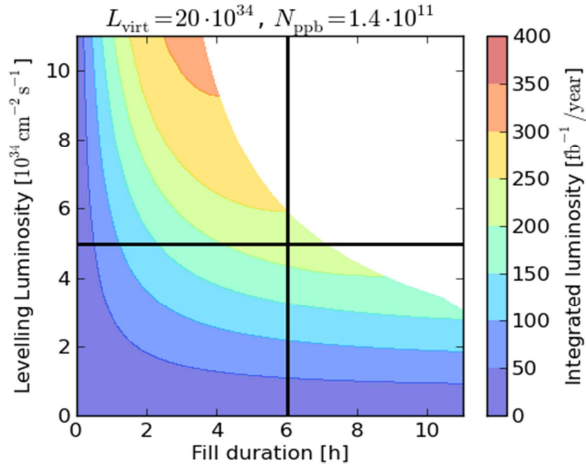
Figure 4: As Fig. 2, but with smaller bunch population than in the baseline scenario. This scenario exploits the conservative region, but it cannot fully profit from long fill durations which are challenging, but not completely excluded. In addition it cannot fully profit from any increase of levelled luminosity.

Optimization Strategy

Figure 2 shows a more realistic case, for which the levelled luminosity is set to $5 \cdot 10^{34}$ cm^{-2}s^{-1}, the virtual luminosity to $20 \cdot 10^{34}$ cm^{-2}s^{-1} and the bunch population to $2.2 \; 10^{11}$ protons per bunch. This case would fully exploit almost all the parameter space and, if the HL-LHC reaches those values of virtual luminosity and bunch populations (representing the baseline values for the HL-LHC), the upgrade project saturates the capabilities of the experiments and should therefore primarily aim at improving the reliability of the machine.

For a limiting case in which, for instance, a high virtual luminosity is not reached at a reasonably high bunch population, for instance without the crab cavities or other mitigation for the geometric reduction factor, most of the parameter space is excluded and also the conservative quadrant can be fully exploited (Fig. 3).

In another limiting case, if the virtual luminosity target is unrealistically achieved without increasing the bunch population, one could see (Fig. 4) that the conservative part of the parameter space is exploited. However, in case the experiments would be able to cope with larger instantaneous luminosities, or the LHC reliability improves enough to allow longer fill duration, the yearly integrated luminosities will not be maximized. This is due to the fact that, while the levelling time depends only on the virtual luminosity, a short luminosity lifetime during the decay time, which depends on the residual bunch population after levelling, has still a detrimental effect in the integrated luminosity. The bunch population target is therefore essential for the HL-LHC project.

This can be seen also, if an even larger virtual luminosity is achieved (Fig. 5) at the cost of a modest reduction of intensity (for instance by reducing β* or by reducing the emittance to the IBS limit) the integrated performance does not improve and tends to limit the potential and robustness of the upgrade.
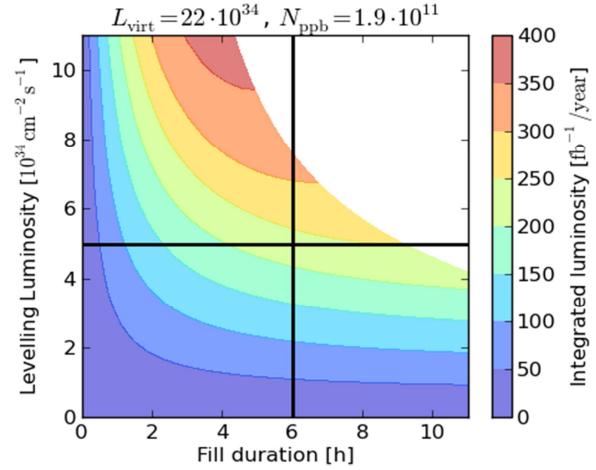

Figure 5: As Fig. 2, but when the virtual luminosity is higher than the ideal scenario at the cost of smaller bunch population (for instance by targeting smaller value β* or by reducing the emittance to the extent allowed by the IBS growth rate). This scenario offers similar features of the baseline one (Fig. 2) but it is inferior for the most aggressive parameters.

From this analysis, one can conclude that the most effective way to optimize the luminosity consists in (besides increasing the efficiency and the days of physics) the maximum levelled luminosity, the fill duration, the bunch intensity and the virtual luminosity. The levelled luminosity is proportional to the number of events per crossing and the present limit is considered extremely challenging to overcome even in the future. Furthermore, the levelled luminosity is proportional to the number of bunches, which are ultimately limited by the bunch spacing (currently limited by both the experiment triggering rate and the e-cloud) and, to a smaller extent, by the rise time of injection, extraction, abort kickers of the LHC and its injectors. The feasibility of an increase of levelled luminosity is not discussed in this paper, but it is under consideration thanks to the possibility that a novel scheme [16] could distribute the events more evenly in the luminous region and therefore ease the event reconstruction.

The remaining part of the paper is devoted to the analysis of the beam parameters and machine scenarios that are needed to achieve the bunch intensity and the virtual luminosity that maximize the HL-LHC performance.

MAXIMIZING THE INTEGRATED LUMINOSITY PER FILL

The way to maximize the luminosity per fill is to maximize the bunch population since the luminosity decay will be dominated by particle burn-off. Efforts should be devoted to keep the sources of emittance growth (instabilities, noise, field imperfections) small. Since the peak luminosity is limited, one should establish a lossless levelling method, which is able to use the reserve performance of a large virtual luminosity. Large virtual luminosities can be achieved by reducing β^* thanks to new large aperture triplets and matching section magnets in addition to an improved orbit control at the IP to avoid jitter larger than a fraction of the transverse beam size. Crab cavities are needed to remove the luminosity reduction due to the crossing angle. The option of flat β^* and LR beam-beam compensators can reduce the crab cavity voltage requirements and, in addition, support the crab kissing scheme [16]. A reduction of the emittance is certainly helpful, however, due to IBS, the gain saturates at values of ~2 μm. In addition, it should not come at extra costs in terms of reduced number of bunches, or exceeding the threshold of head-on beam-beam tune shift and instabilities.

Since the maximum levelled luminosity depends also on the peak pile-up line density, it is desirable to use long bunches (limited by the RF control, crab cavity RF curvature and hour-glass effect), flat longitudinal density (by a 2nd harmonic RF), and to have enough crabbing kick to support the crab kissing scheme.

The following sections will sketch the challenges associated with the strategy mentioned above.

Beam current limitations

The present understanding (see Fig. 6, 7) indicates that it should be possible to maintain in collisions $2.2 \cdot 10^{11}$ protons per bunch for a total of about 1 A circulating current [17]. This scenario requires that the e-cloud issues are under control (see following subsection), that the coupled bunch instabilities are stabilized by the transverse damper and that the single bunch instabilities have a threshold in agreement with predictions (see Fig. 8) or are stabilized by the head-on beam-beam tune spread [18, 19].
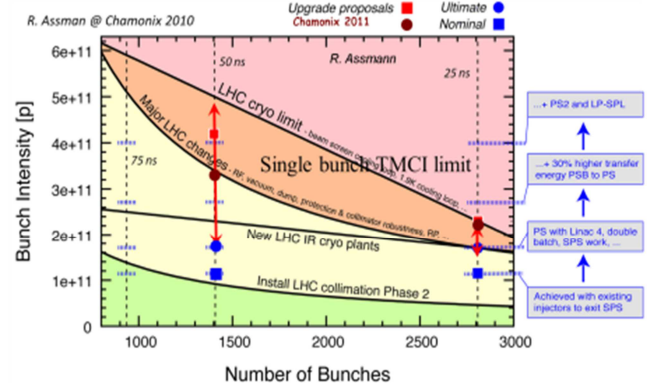

Figure 6: Beam current limitation in the LHC as a function of bunch intensity and number of bunches (courtesy R. Assmann [17]).
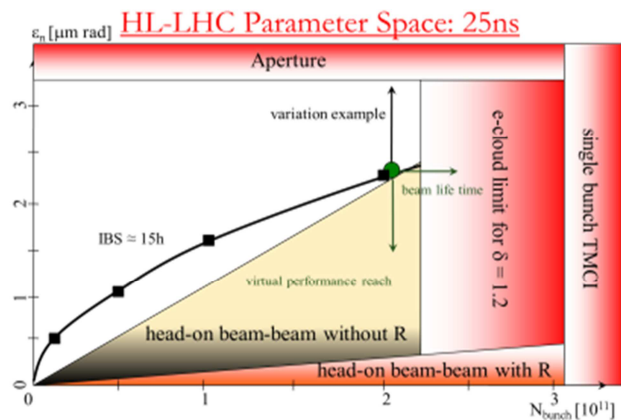

Figure 7: Parameter space of 25 ns beams in terms of emittance and bunch intensity. For large intensity the area is bounded by the e-cloud limit and IBS growth rate if the performance reach is maximized.
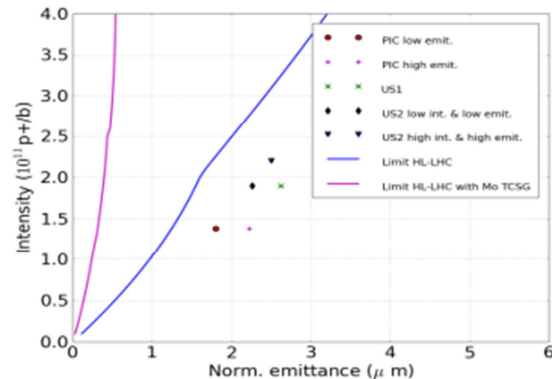

Figure 8: Instability thresholds are still far according to the present impedance model (bottom [19]) if metallic collimators are implemented.

E-cloud

As stated above, the HL-LHC nominal scenario relies on the control of e-cloud issues. The current understanding, based on the observations performed during Run I and on numerical simulations, indicates that by scrubbing the main dipoles until reaching a secondary emission yield (SEY) of 1.3-1.4, one could alleviate the heat-load and emittance growth at injection energy. In addition, it should be possible to increase the cryogenic cooling capacity in the quadrupoles to cope with the heat-load since the required SEY smaller than 1.2, 1.3 (see Figure 9) would be difficult to achieve with scrubbing [20].
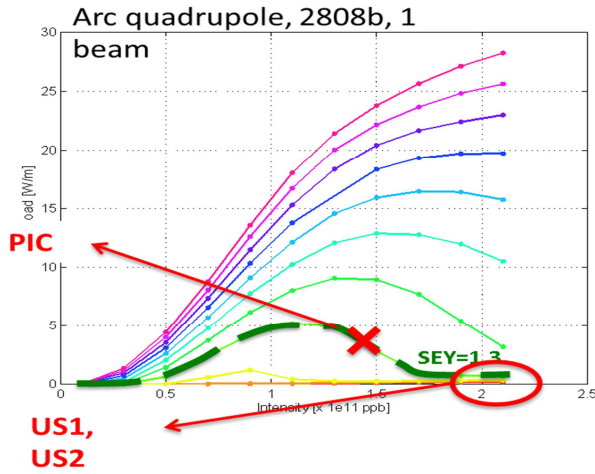

Figure 9: Simulated heat load linear density in the LHC arc quadrupoles as a function of bunch population and SEY. A SEY of 1.3 is needed to reduce the heat load [20].

Filling schemes

The number of bunches is one of most sensitive parameters to gain in performance, because it is proportional to the instantaneous luminosity. The filling schemes in the accelerator chain, the maximization of the colliding bunches for the four experiments, and the need of non-colliding bunches affect the total number of the colliding bunches that would be otherwise limited only by the rise and flat top time of the LHC injection kickers (0.925 μs and 7.86 μs), the rise time of the dump kickers (3 μs), and the 4-fold symmetry to 2808 bunches [21]. Two SPS injection schemes, a standard 72-bunch one and the Batch Compression Merging and Splitting (BCMS) scheme [22] for 48 high brightness bunches, allow to inject in the LHC 2592 and 2736 colliding pairs in both ATLAS and CMS, while keeping a fair number of collisions for ALICE and LHCb (see Fig. 10 and Table 1 [23]). These schemes feature no IP8 private bunches that

might be lost (in particular if colliding with large separations) since they will have only the tune spread of one head-on collision to stabilize instabilities due to impedance effects.

The small difference in number of colliding bunches for the two schemes is nevertheless significant in the performance evaluation due to the steeper increase of integrated performance originating from a higher levelled luminosity compared to the gain from higher virtual luminosity that contributes only to the length of the fill.
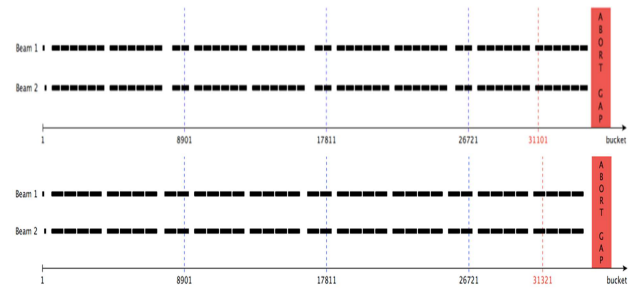

Figure 10 and Table 1: HL-LHC filling schemes for standard 72 bunch injection and BCMS injection featuring 12 non-colliding bunches and no IP8 private bunches [23].

Filling scheme	Total	IP1-5	IP2	IP8
BCMS: 48 b 6 PS injections, 12 SPS injections	2604	2592	2288	2396
Standard: 72 b 4 PS injection, 12 SPS injection	2748	2736	2452	2524

Experimental constraints and levelling

The HL-LHC baseline scenario aims at saturating the capabilities of the high luminosity detectors as long as possible. The limits on data taking for the HL-LHC detectors are not yet fully explored. Some of the conditions to be taken into account are the total pile-up, pile-up density, out of time pile-up or spill-over, centroid movements and size changes of the luminous region, and instantaneous luminosity stability [24].

Regardless of the maximum instantaneous luminosity, the machine needs to establish a method to reduce artificially the luminosity when the bunch population is the largest and to modify slowly those conditions that increase the luminosity with decreasing bunch population. The methods should take into account that the orbit stability should be a small fraction of sigma to avoid beam losses and in particular in the last part of the fill to avoid the reduction of the overlap between bunches of the two beams.

Several methods have been identified: β* levelling, parallel separation, bunch tilt. In case of β* levelling, one has a large range of luminosity reduction and it is the preferred option for ATLAS and CMS. It has the advantage of reducing the impact of the long range beam-beam encounters when the bunch population is large. However, this method relies on the simultaneous modification of the optics and orbit, and it implies a large head on beam-beam tune spread. Both operations rely on a combination of high reproducibility of the magnetic cycles, accurate transfer function models and high precision, accuracy and resolution of the BPMs and power converter controls. In addition, since the HL-LHC optics needs the ATS scheme (discussed later), the preparation of the squeeze sequence is complicated if both CMS and LHCb undergo β* levelling at the same time.

Alternatively, a reduction of luminosity is possible by parallel separation. In this case the head-on tune spread reduces. On one hand, this mitigates the beam–beam related lifetime issues if they are a limiting factor, but, on the other hand this would limit the largest source of Landau damping if it is needed to stabilize instabilities. In addition the parallel separation may enhance beam-beam driven coherent effects. By increasing the crossing angle with the orbit correctors or the bunch tilt with crab cavities, one can have the beneficial effects of the parallel separation without enhancing coherent effects (at the cost of larger synchro-betatron resonances). However, the range is too limited to cover the needs set by the bunch population assumed for the discussed scenarios due to aperture and crab cavity voltage constraints for the crossing angle and bunch tilt respectively.

Optics for reaching low β*

The nominal transverse beam size at the IP (proportional to $\sqrt{\beta^*}$) is not sufficiently small to reach the peak luminosity needed by the HL-LHC baseline. The further reduction of β* is obtained by the replacement of the inner triplet (that would however have to be replaced after 300 to 600 fb^{-1} of equivalent radiation damage dose) in combination with the implementation of the so-called Achromatic Telescopic Squeezing scheme [25]. The principle of this novel scheme is to extend the optics matching of the high luminosity insertions to the neighbouring arcs and straight sections in order to mitigate the strength limits of the matching quadrupoles (needed for the optics squeeze) and of the arc sextupoles (necessary for the chromatic aberrations generated by the stronger focusing) [26]. The scheme has already been successfully tested for β* as low as 10 cm using pilot bunches ([27] and Fig. 11) and represents a solid base

around which the lattice hardware modification are being tailored [28].
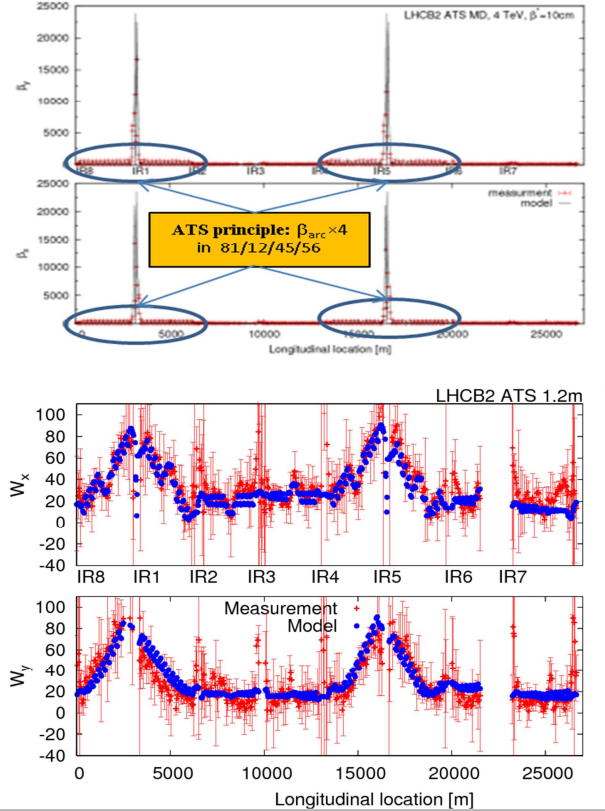

Figure 11: Telescopic optics functions and achromatic matching of the first order chromatic perturbations of the LHC as measured during a machine test demonstrating the feasibility of this optics scheme in view of the HL-LHC [27].

Crab cavities for performance boost

The presence of a crossing angle reduces both the peak luminosity and the size of the luminous region, thus enhancing the pile-up density and at the same time diminishing the constant luminosity. Crab cavities would be able to tilt the bunch at the IP and therefore mitigate those effects ([29] and Figure 12). Explicitly a gain of 68 % or 41 % in peak luminosity, 13 % and 6 % in integrated performance, and 2.7 and 1.7 reduction of pile-up density for round and flat β* ratio, respectively could be achieved.
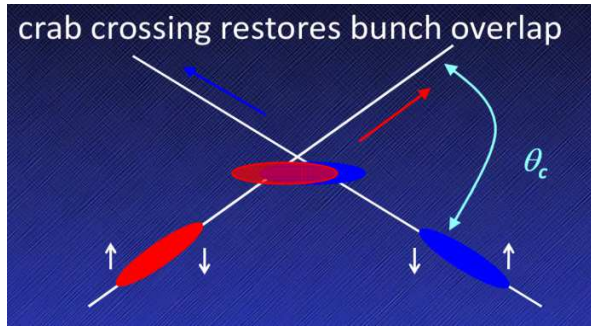
Figure 12: Principle of crab bunch tilting.

The voltage required assuming three or four cavities per beam and side is about 12 MV for round optics. The ideal location for the installation is in between D2 and Q4 on the left and right side of Point 1 and 5 in order to maximise the effect and making the tilt as local as possible [28]. Different cavity designs (Fig. 13) have been studied in parallel and first cold test showed very promising results for obtaining the desired voltage.
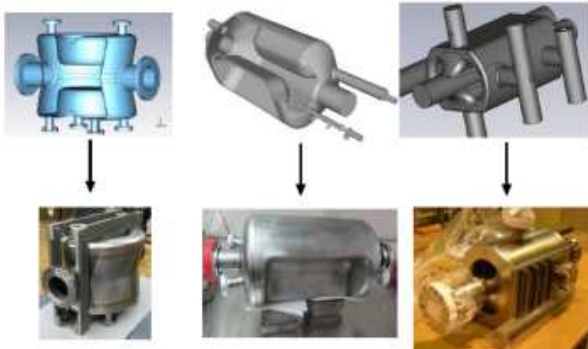

Figure 13: Crab cavity design and prototypes being studied and tested for the LHC [29].

Since these devices have never been used in hadron colliders, considerable effort is put in evaluating the failure scenarios (e.g. loss of a cavity) and the operational aspects (e.g. noise control). A test with beam is foreseen in the SPS that would validate the manufacturing aspects, the peak voltage consistency and the operational issues with beam.

Moreover, the tilting effect can also be used to reduce substantially the peak line density, thanks to the crab kissing scheme [16].

HL-LHC Baseline layout

The replacement of the inner triplets with large aperture Nb$_3$Sn counterparts is part of a large hardware modification that is needed for optics matching, radiation protection, and collimation improvements. The following interventions are foreseen (see Fig. 14 and 15) [30]:

- new 150 mm, 140 T/m Nb$_3$Sn triplets for aperture [30] and a superferric non-linear corrector package [31];
- cold 150 mm Nb-Ti D1 [32];
- new TAN-D2-Q4-Q5 with strong orbit correctors for compact crossing, and separation scheme bumps: for aperture, optics flexibility [33], and crab cavity integration [34];
- new TCL and TCT collimators for debris and protection [35];
- three or four crab cavity modules for beam tilt angle control [29];
- 4 additional 2-in-1 MS sextupoles in Q10 around IP1 and IP5 and stronger Q5 in Point 6 in order to exploit the full ATS potential [33];
- superconducting links to connect surface host power converter in order to reduce radiation related faults [36];
- wires for long-range beam-beam compensation [37].

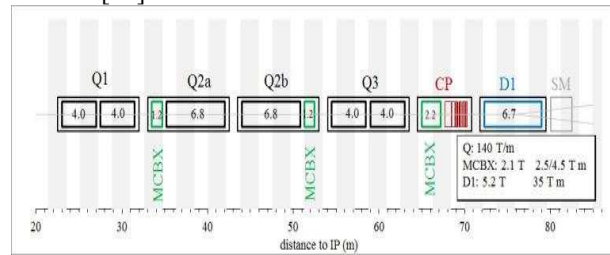Figure 14: Schematic view of the new inner triplet region foreseen for the HL-LHC in Point 1 and 5.
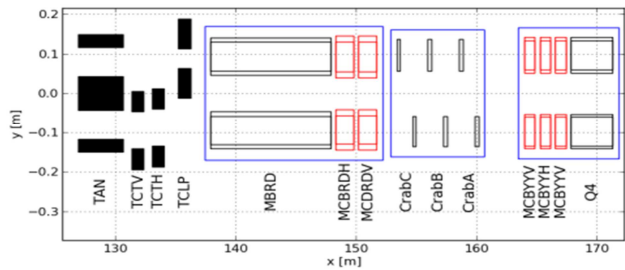

Figure 15: Schematic view of TAN - crab cavities - Q5 region foreseen for the HL-LHC in Point 1 and 5.

With the present layout and thanks to the ATS scheme, the HL-LHC aims at a baseline β* of 15 cm for round optics and 7.5 cm in the non-crossing plane (with 30 cm in the crossing plane) for flat optics.

Radiation protection of high luminosity areas

Several protection devices are being implemented to keep the radiation impact on the elements in the high luminosity regions at acceptable levels, despite the accumulated and instantaneous luminosity targets which are 10 times and 5 times higher than the ones of the nominal LHC, respectively.

Inner triplets have Tungsten inserts along their length to reduce the peak dose in the magnet to a similar level as that of the nominal triplets (about 2-3 mW/cm^3 at $5 \cdot 10^{34}$ cm^{-2}s^{-1} and below 25 to 35 MGy after 3000 fb^{-1} [38], see Fig. 16).
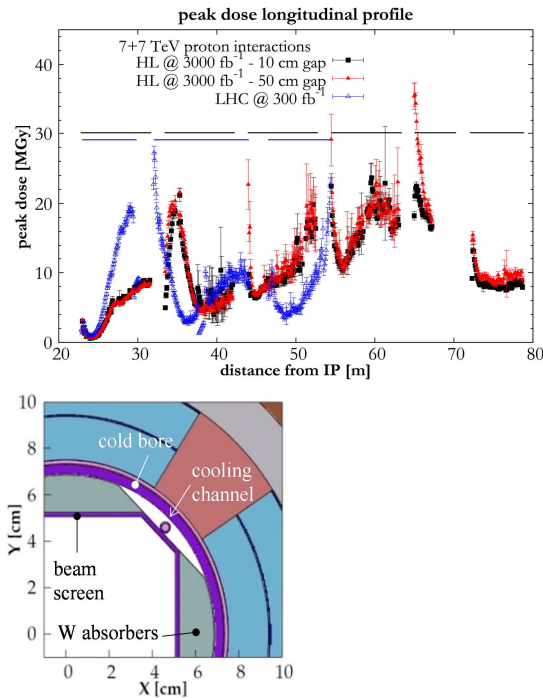

Figure 16: Simulated peak dose in the triplet area for the HL-LHC and LHC (top, [38]) and sketch of the cross section of a part of the inner triplet highlighting the W insert (bottom). The gap in between the triplets (50 cm), which is hosting the BPMs, could be reduced (e.g. 10 cm) by filling with the same high Z material inserts the region in between the couplers, which would result in a reduction of the peak dose from 35 MGy to 25 MGy, equivalent to what is expected for the LHC before the HL-LHC upgrade (LS3).

A new TAN, fixed W masks in front of D2, Q4, Q5 and additional TCLs are considered to protect the matching section (below 1 mW/cm^3 at $5 \cdot 10^{34}$ cm^{-2}s^{-1} and below 25 MGy after 3000 fb^{-1} [39] could be ideally reached if the mask are sufficiently long and close to the sensitive

devices, see Fig. 17). Detailed studies are being carried out on a realistic mechanical design for an accurate validation of the protection strategy.
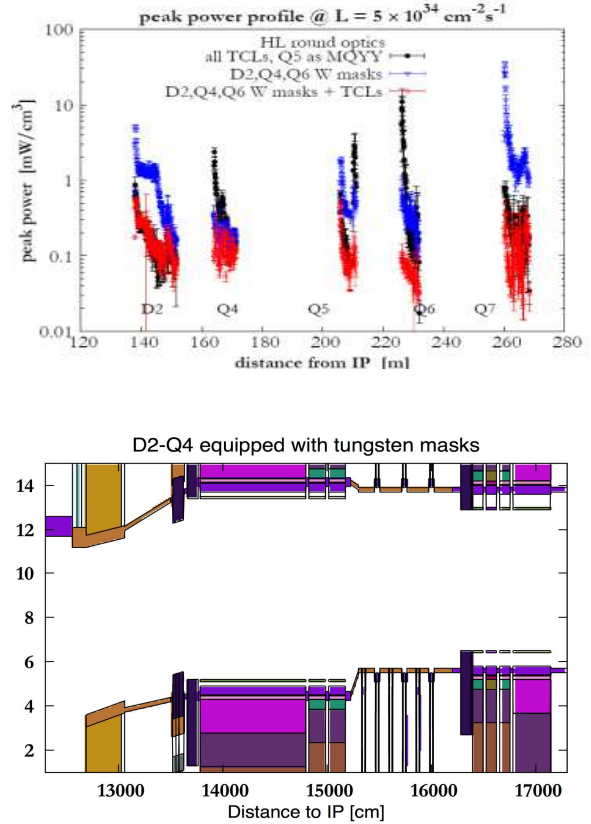

Figure 17: Simulated peak power deposited in the matching section cold magnets foreseen for the HL-LHC and LHC (top [39]) and sketch of a detail of the cross section of the TAN-Q4 area (bottom).

Collimation and aperture protection

The collimation system will face the challenge posed by twice the nominal stored beam energy, while trying to reduce as much as possible the aperture tolerances in order to achieve the lowest β* possible. The collimation system consists of a large number of devices ordered in a strict hierarchy. Closest to the beam are the primary and secondary collimators in Point 7, used for global cleaning. Other important collimators are TCS and TCDQ in Point 6, which should protect the machine in case of asynchronous dumps, and the tertiary collimators in Point 1, 5, 2, 8 that should protect the local aperture bottlenecks and reduce experimental background.

The minimum primary collimator aperture is practically determined by: the impedance budget, the ability to control the orbit to avoid loss spikes and protection during

failure scenarios (e.g. asynchronous dumps). Based on these different points the following upgrades are planned [40]: metallic collimators or equivalents for impedance reasons (if compatible with the required robustness), button BPMs at all jaws for accurate and fast alignments and reduced margins, and possibly an e-lens [41] to control the halo population, mitigate loss spikes and possibly for machine protection in case of failure of the crab cavities. Even after the foreseen upgrade, the collimator settings, which define the minimum protected aperture and therefore the β^* reach, practically do not scale with the beam emittance, as it would be the case if the collimation settings were determined by lifetime considerations when cutting into the beam only. While detailed cleaning efficiency and loss map simulations will define a solid scenario and collimator settings, a tentative proposal has been developed (see Table 2) to establish the β^* reach [42].

Table 2: Aperture of the collimator jaws, expressed in terms of σ calculated with the arbitrary value of 3.5 μm normalized emittance. Values from the LHC design report and HL-LHC first guess are compared.

Aperture at 3.5 μm 7TeV	LHC Design	HL-LHC
TCP IR7	6.0	5.7
TCS IR7	7.0	7.7
TCS IR6	7.5	8.5
TCDQ IR6	8.0	9.0
TCT IR1/5	8.3	10.5
Min. Aperture IR1/5	8.4	12

At the same time operational margins of orbit control, beta-beating correction, dispersion correction and off-momentum errors are being reviewed in order to qualify the aperture margins. Table 3 shows the last proposal based on experience and non-conformities [43].

Table 3: Operational margin proposed for the HL-LHC aperture evaluations.

Parameter	LHC Design	HL-LHC
Closed orbit excursion	3 mm	2 mm
Beam size change from β-beat	1.1	1.1
Normalized emittance	3.75 μm	3.5 μm
Momentum offset	$8.6\ 10^{-4}$	$2\ 10^{-4}$
Relative parasitic dispersion	0.27	0.1

Beam-beam effects and crossing angle

In general, beam-beam effects are enhanced by bunch population and for the head-on interaction by small emittances. Concerning head-on effects, the maximum tune spread tolerated by the machine is not known at the moment, although the machine has been running without lifetime degradation at injection energy and without crossing angle (large β^*, no long range interaction) with a beam-beam parameter of 0.034. However, three collision points at full intensity with crab crossing are considered very challenging in this respect. The long-range effects limit the minimum crossing angle expressed in beam sigma separations. For the nominal LHC, 10 σ separation was considered as a safe assumption, while for the HL-LHC one would need between 12 σ for round β^* and 15 σ for flat β^* aspect ratio (Fig. 18) due to the enhanced bunch population, the larger number of long range interactions and the higher beta functions [25]. These values translate to 590 μrad full crossing angle for round $\beta^* = 15$ cm and 540 μrad for flat $\beta^* = 7.5/30$ cm.
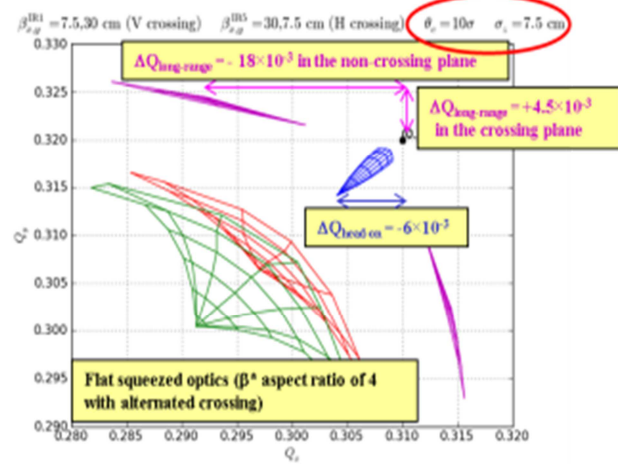

Figure 18: Illustrations of the different contributions of the beam-beam force to the tune footprint for flat beam aspect ratio [25].

In order to reduce the crossing angle with the aim of gaining aperture and reducing the voltage in the crab cavities, a long range beam-beam compensation device (for instance high current wires located close to the interactions) is foreseen to be installed. It is assumed that with this device it would be possible to reduce the required beam separation to 10 σ for both round and flat β^* aspect ratios. The minimum beam separation depends also on the luminosity leveling scheme. If β^* leveling is used, the minimum separation would not occur at maximum bunch population but at about $1.2\ 10^{11}$ proton per bunch (see Fig. 19). Effects like Pac-man bunches and minimum dynamic aperture in the presence of other field imperfection is under study.
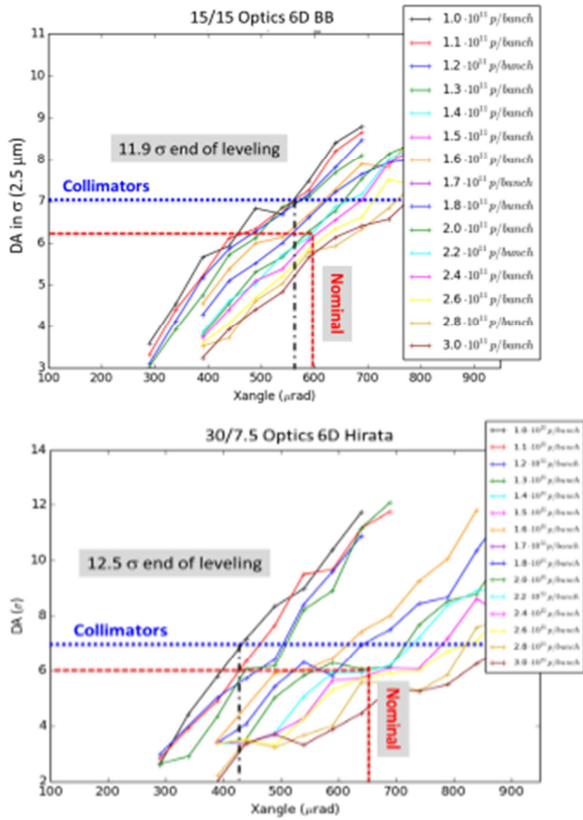
Figure 19: Scan of the dynamic aperture as a function of the crossing angle for round (top) and flat β* (bottom) aspect ratios and bunch population without wire compensation [44, 45].

Injection to collision transmission efficiencies

The beam parameters needed by the HL-LHC exceed the present capabilities of the injector chain. The LHC Injector Upgrade (LIU) project contains all the activities of consolidation and upgrade needed to produce the beam to be injected in the HL-LHC [2]. The beam parameters at LHC injection are related to the ones at collision by a budget of beam losses and emittance growth that are assumed to be 5 % and 20 % respectively. The processes that cause these losses have different sources: injection mismatch, noise, e-cloud, intra beam scattering (IBS) and non-linear diffusion. The IBS effect on the emittance growth has been evaluated by assuming a scenario of ramping time, RF voltage and longitudinal emittance and calculated as a function of bunch population and emittance (see Fig. 20 and [46]).

Three scenarios [47] have been considered with different trade-off between intensity and emittance (see Table 4). The first two correspond to the best performance that the LIU project is confident to deliver for the BCMS filling scheme "LIU-BCMS" and the standard scheme "LIU-STD", respectively. The last corresponds to the ideal parameter set for the HL-LHC. The LIU-BCMS offers very high brightness that however cannot be preserved due to the large emittance growth. This option implies also a smaller number of bunches, which makes it less attractive when the overall performance is considered (see following paragraph). The LIU-STD is still compatible with the emittance growth budget; however it does not reach the desired bunch population. The last option is well within the budget and offers the best integrated performance.
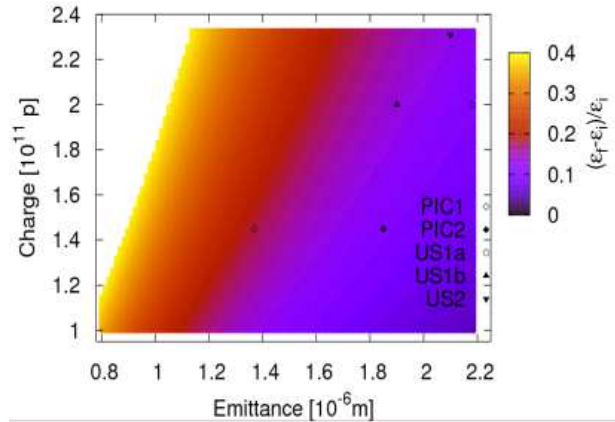

Figure 20: Emittance growth between injection and collision due to IBS. For the intensities needed by the HL-LHC baseline scenario the low value of emittance cannot be transmitted within the foreseen budget.

In order to validate the cycle scenarios it is important to know at which point of the cycle and in which location the beam losses occur (e.g. transfer lines, septa, TDI or the LHC) since the can sustain 5% losses only if evenly spread in time. Concerning the emittance growth - since most of the margin are used by IBS - one has to control the additive sources (e.g. noise, injection errors) of blow-up and the blow-up due to electron cloud, to reduce the impedance with metallic collimators, and support long bunches (10 cm) till stable beams to mitigate the IBS effects.

Table 4: Beam parameters at SPS extraction and at the LHC in collision expected for three cases. The brightest one (LIU-BCMS) exceeds the IBS budget. The underlying model does not assume any horizontal/vertical coupling; therefore the blow-up is only in the horizontal plane. The percentage corresponds to emittance blow-up from injection to collision. In the RLIUP scenarios a budget of only 20% is assumed in both planes and therefore the LIU-BCMS expected emittance exceed this value. This implies that larger emittance (1.85 μm) should be more realistically considered for a fair comparison.

Scenario	SPS Extraction		LHC Collision Minimum value from IBS	LHC collision Assumed	
	Bunch population $[10^{11}]$	$\varepsilon_{n\,inj}$ [μm]	$\varepsilon_{n\,coll.\,(H/V)}$ [μm]	Bunch population $[10^{11}]$	$\varepsilon_{n\,coll.}$ [μm]
LIU-BCMS	2.0	1.37	1.78(30%)/1.37	1.9	1.65
LIU-STD	2.0	1.88	2.20(17%)/1.88	1.9	2.26
HL-LHC	2.31	2.08	2.41(15%)/2.08	2.2	2.5

PERFORMACE EVALUATION OF THE HL-LHC SCENARIO

Previous sections highlighted the boundary conditions, the challenges, the upgrade plans and the open questions related to optimization of the HL-LHC performance. This section illustrates quantitative estimates of several operating scenarios and validates the choices of which parameters are to be optimized.

The analysis is carried out by evaluating the differential evolution of an ideal fill including the effect of burn-off, IBS emittance blow-up (plus an additional 200 h in the vertical plane to fit the 2012 experimental data) and radiation damping. The results of the ideal fill are extrapolated in order to obtain the required performance efficiency necessary to achieve the yearly integrated luminosity goal. Table 4 shows the parameters that are constant for all scenarios. A bunch length of 10 cm has been used to mitigate the pile-up density; however the nominal 7.55 cm would be more beneficial for the hour-glass effect and the RF curvature.

Table 4: Parameters that are assumed in the evaluation of the integrated luminosity of ideal fills.

"Visible" cross-section IP1-5/8 [mb] for pile-up estimation	85/75
Pile-up limit IP1-5/8	140/4.5
Luminosity limit IP2 $[10^{34}$ cm^{-2} s$^{-1}]$	0.002
Energy [TeV]	6.5 or 7
Total RF Voltage	16
Long. emit.ε_L*[eV.s] at start of fill	3.8
Bunch length (4 s)[ns]/ (r.m.s.) [cm]	1.33/10

The typical evolution of the simulated luminosity in ATLAS and CMS during a fill is shown in Fig. 21. The luminosity is levelled until β* reaches the minimum value allowed by the aperture of the inner triplets. The bunch population decays almost always linearly as the instantaneous luminosity is constant. The longitudinal emittance decays due to radiation damping and the transverse emittance is in equilibrium thanks to the balance between the growth due to IBS and noise and synchrotron radiation damping.

The β* evolution is also linked to the beam-beam separation (see Fig. 22) around the IP since the crossing angle is physically unchanged during the fill. When the luminosity is constant the length of the luminous region decreases, and therefore the longitudinal pileup density increase, because the geometric reduction factor reduces with β* at constant crossing angle. As soon as the luminosity starts to decay and β* is constant, the pileup density decays as well.
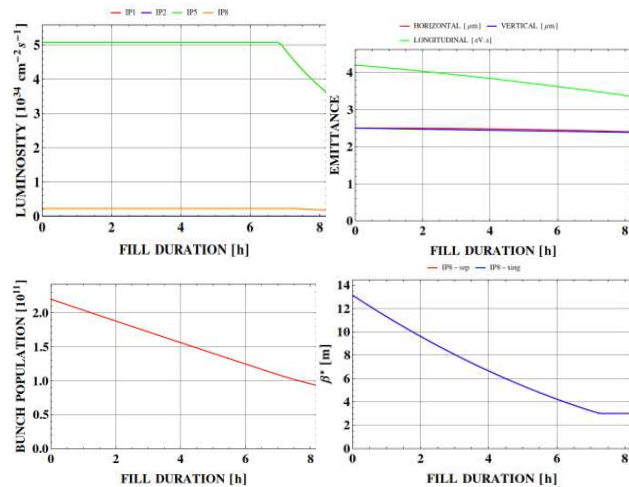

Figure 21: Luminosity (top left), emittance (top right), bunch population (bottom left), β* evolution (bottom right) as a function of time for an ideal fill of the HL-LHC baseline round scenario.
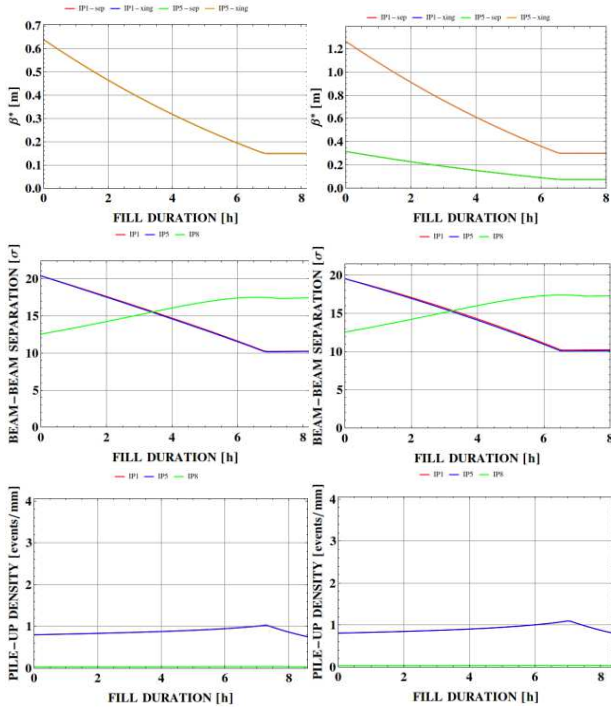
Figure 22: Evolution during an ideal fill of β* (top), beam-beam separation (middle) and pile-up density (bottom) as function of time for an ideal fill of the HL-LHC round (left) and flat (right) scenarios, respectively.

8) by calculating the integrated luminosity of an ideal fill, the maximum yearly integrated luminosity and the yearly integrated luminosity assuming a fill length of 6 hours. The maximum and 6 hour-fill yearly integrated luminosity is translated in the efficiency required to reach the target of 270 fb^{-1}, respectively η_{6h} and η_{opt}.

The first scenario, labelled RLIUP2, is characterized by a fairly large virtual luminosity obtained by very small transverse emittance and comparably small bunch population. The integrated performance is the worst of the set because the low intensity cannot produce long enough fills and the effect of IBS reduces very quickly the virtual luminosity over time.

Scenario LIU-BCMS is produced by the BCMS scheme and full LIU upgrade and neglecting the part of emittance growth due to the IBS (see Table 3). This scenario offers the largest virtual luminosity, however overall performances are degraded by the lower number of bunches and the IBS effects (slightly underestimated in the table since the starting emittance should be higher to be consistent between the scenarios with a common additive emittance blowup in addition to the IBS effects).

Scenario LIU-STD is produced by the standard production scheme and the full LIU upgrade. This scenario, while having a smaller virtual luminosity, results in larger integrated performance compared to the previous one thanks to the higher number of bunches and the resulting higher levelled luminosity.

Using the differential evolution, several beam parameter scenarios have been evaluated (see Table 7 and

Table 7: Parameters and estimated peak performance for several options at 6.5 TeV. [1] Flat beams are also compatible with the crab kissing scheme. [2] Long range beam-beam compensators are assumed to allow reducing the crossing angle to 10 σ, otherwise the crossing angle in parenthesis would be needed. [3] These values of β* are assumed to be possible thanks to the reduction of the crossing angle for the same aperture margins of the nominal round beam case. 4) The value of β* can be reached only with LHC design collimator settings. [5] Scenarios evaluated with a pile-up limit of 200 events per crossing. [6] The starting value of the emittance is not compatible with both the IBS blow-up from injection to collision and the otherwise assumed 20% margins. A value of 1.86 µm (30% blow-up) is more likely.

	N_b coll	$\varepsilon_{n,}$ coll	β* (ing/ sep)	Xing angle	n_{coll} IP1,5	L_{peak}	L_{lev}	t_{lev}	t_{opt}	η_{6h}	η_{opt}	Avg. Peak pile-up Density
	10^{11}	µm	cm	µrad		10^{34} cm^{-2}s^{-1}	10^{34} cm^{-2}s^{-1}	h	h	%	%	ev./mm
RLIUP2	1.5	1.3[6]	15	366	2592	17.6	4.8	4.4	5.8	64.6	64.6	0.88
LIU-BCMS	1.9	1.65[6]	13.5[3]	420	2592	21.7	4.8	6.3	7.5	61	58.4	0.94
LIU-STD	1.9	2.26	14.5[3]	474	2736	15.8	5.06	5.3	6.9	58.2	57.5	0.97
HL-Flat	2.2	2.5	30/ 7.5[1]	348[2] (550)	2736	17.2	5.06	6.5	8.0	57.8	54.5	1.05
HL-Round	2.2	2.5	15	490[2] (590)	2736	18.7	5.06	6.8	8.2	57.8	54	1.05
LIU-BCMS	1.9	1.65	13.5[3]	420	2592	21.7	6.87[5]	4.3	6.2	52.2	52.2	1.34
HL-Round	2.2	2.5	15	490	2736	17.2	7.24[5]	5.4	7.3	48.8	48.4	1.37
HL-SRound	2.2	2.5	10[4]	600	2736	18.7	7.24[5]	4.4	6.7	47.7	46.4	1.55

Table 8: As Table 7, but computed at 7 TeV. Performance increase with respect to 6.5 TeV thanks to the reduction of the geometrical emittance and the increase of radiation damping better mitigating the blow-up due to the IBS.

	N_b coll	$\varepsilon_{n,}$ coll	β^* (xing/ sep)	Xing angle	n_{coll} IP1,5	L_{peak}	L_{lev}	t_{lev}	t_{opt}	η_{6h}	η_{opt}	Avg. Peak pile-up density
	10^{11}	µm	cm	µrad		10^{34} $cm^{-2}s^{-1}$	10^{34} $cm^{-2}s^{-1}$	h	h	%	%	ev./mm
RLIUP2	1.5	$1.3^{6)}$	15/15	341	2592	19	4.8	4.7	6	63.4	63.4	0.94
LIU-BCMS	1.9	$1.65^{6)}$	$13.5^{3)}$	405	2592	23.4	4.8	6.7	7.8	61	57.5	0.98
LIU-STD	1.9	2.26	$14.5^{3)}$	457	2736	17	5.06	5.7	7.2	58.2	56.4	1.01
HL-Flat	2.2	2.5	30/ $7.5^{1)}$	$335^{2)}/$ 550	2736	18.6	5.06	7	8.4	57.8	53.5	1.12
HL-Round	2.2	2.5	15/15	$476^{2)}/$ 590	2736	20.1	5.06	7.3	8.6	57.8	53.1	1.03
LIU-BCMS	1.9	1.65	$13.5^{3)}$	579	2592	23.4	$6.87^{5)}$	4.6	6.4	51.4	51.3	1.34
HL-Round	2.2	2.5	15/15	473	2736	20.1	$7.24^{5)}$	4.8	7	48.2	47.4	1.37
HL-SRound	2.2	2.5	$10^{4)}$	600	2736	26.8	$7.24^{5)}$	5.8	7.6	47.6	45.7	1.55

Scenarios HL-Flat and HL-Round represent the HL-LHC baseline and offer the best performance and are identical besides the difference in the β* values. Flat optics allows for a smaller voltage from the crab cavities, but relies on beam-beam long range compensation to avoid increasing the crossing angle too much. Also beam-beam effects with unequal beam sizes need to be validated. Round optics require a larger crab cavity voltage. Long range beam-beam compensation, while helpful to reduce the crossing angle, is not as critical as for the flat option. The last set of scenarios assumes that the maximum levelled luminosity could be increased such that the maximum number of pile-up events is 200. In this case, the yearly performance of LIU-STR and HL-Round increases, but only HL-Round can reach the performance goal with efficiency below 50%. The reason is that the higher bunch population, as discussed earlier in this paper, gives more margins for aggressive boundary conditions.

SUMMARY AND CONCLUSIONS

The HL-LHC integrated luminosity expectations are bounded by the capabilities of the experiments in using large instantaneous luminosity. Once the maximum level is established, one has to operate the LHC with the beam parameters and the reliability that allows keeping the maximum accepted luminosity as long as possible. Assuming $5 \cdot 10^{34}$ $cm^{-2}s^{-1}$, fills as long as 10 hours are needed to approach the performance goal of 270 fb^{-1} per year or 3000 fb^{-1} by 2035 with performance efficiency close to those achieved in 2012. The maximum number of colliding bunches of 2736, a bunch population of 2.2 10^{11} and a virtual luminosity of $20 \cdot 10^{34}$ $cm^{-2}s^{-1}$ allow to exploit most of the parameter space and give margins either for pushed levelled luminosity or overall robustness against unexpected issues. The full LIU upgrade, the solution of the e-cloud issues and the control of impedance are needed to support a large bunch population. The virtual luminosity is obtained by upgrading the inner triplet and MS magnets to be able to reduce β* thanks to the ATS scheme, and by installing crab cavities and long-range wire compensators to eliminate the geometric reduction factor. Increased radiation levels need to be addressed with a redesign of the TAN-D2-Q4 region. Critical open questions besides the e-cloud are how to establish lossless operations of luminosity levelling and how to drastically reduce the number of unwanted beam dumps.

ACKNOWLEDGEMENTS

REFERENCES

[1] L. Rossi, "LHC Upgrade Options and Plans", in Proceedings of IPAC2011, San Sebastian, Spain, http://cern.ch/HiLumiLHC.

[2] R. Garoby, "Plans for the upgrade of the LHC injectors", in Proceedings of IPAC2011, San Sebastian, Spain, http://cern.ch/liu-project.

[3] S. Myers, F. Bordry, "Review of the LHC and Injector Upgrade Plans Workshop", Archamps, 29th-31st October, 2013, http://indico.cern.ch/conferenceDisplay.py?confId=260492.

[4] M. Meddahi, L. Rossi, "Adding Performance improving consolidation", RLIUP, Session 3A, Archamps, 29th-31st October, 2013, http://indico.cern.ch/sessionDisplay.py?sessionId=3&confId=260492#20131030.

[5] M. Meddahi, L. Rossi, "Upgrade scenario 1", RLIUP, Session 3B, Archamps, 29th-31st October, 2013,

http://indico.cern.ch/sessionDisplay.py?sessionId=2&confId=260492#20131030.

[6] G. Goddard, R. Garoby, "Upgrade scenario 2", RLIUP, Session 4, Archamps, 29th-31st October, 2013, http://indico.cern.ch/sessionDisplay.py?sessionId=4&confId=260492#20131030.

[7] M. Lamont, "Integrated luminosity scenarios", 6th HL-LHC Coordination Group meeting, 25/7/2013, https://indico.cern.ch/getFile.py/access?contribId=8&resId=0&materialId=slides&confId=264629.

[8] G. Arduini, et al., "PICS: what do we gain in beam performance", these proceedings.

[9] J. Wenninger, "Integrated performance of the LHC at 25 ns without and with LINAC4", these proceedings.

[10] B. Di Girolamo, "Detector Limits", these proceedings.

[11] R. Jacobsson, "Plans and physics outlook for non-high luminosity experiments until and after LS3", these proceedings.

[12] G. Antchev et al., "Luminosity-independent measurements of total, elastic and inelastic cross sections at $\sqrt{s}$=7 TeV", CERN-PH-EP-2012-353.

[13] G. Antchev et al., "Luminosity-independent measurements of the proton-proton total cross section at $\sqrt{s}$=8 TeV", CERN-PH-EP-2012-354.

[14] B. Gorini, private communication.

[15] F.Zimmermann, "New ideas", HL-LHC/LIU Joint Workshop, CERN, 30 March 2012, https://indico.cern.ch/contributionDisplay.py?contribId=4&confId=175259.

[16] S. Fartoukh, "Pile-up at HL-LHC and possible mitigation", ECFA High Luminosity LHC Experiments Workshop, 1st October 2013, Aix-les-Bains, France, http://indico.cern.ch/materialDisplay.py?contribId=14&sessionId=5&materialId=slides&confId=252045.

[17] R. Assmann, "Implications of higher intensities in the LHC", Proceedings of Chamonix 2010 workshop on LHC Performance.

[18] O. Bruning, "HL-LHC Parameter Space and Scenarios", Proceedings of Chamonix 2012 workshop on LHC Performance.

[19] E. Métral, N. Mounet, "Update on stability limits and collimator impedance upgrade needs", 20th Hi-Lumi Work Package 2 Task Leaders' Meeting, 25/10/2013, https://indico.cern.ch/getFile.py/access?contribId=4&resId=0&materialId=slides&confId=278765.

[20] G. Rumolo, "Update on Electron Cloud", presentation at the 169th LHC Machine Committee, https://espace.cern.ch/lhc-machine-committee/Presentations/1/lmc_169/lmc_169e.pdf.

[21] R. Bailey, P. Collier ."Standard Filling Schemes for Various LHC Operation Modes", LHC-Project-note-323.

[22] H. Damerau, A. Findlay, S. Gilardoni, S. Hancock, "RF manipulations for higher brightness LHC-type beams", WEPEA044, IPAC 2013.

[23] B. Gorini, private communication.

[24] R. Jacobsson, "Needs and requirements from the LHC physics experiments", Proceedings of ICFA Mini-Workshop on Beam-Beam Effects in Hadron Colliders, CERN, March 2013, https://indico.cern.ch/getFile.py/access?contribId=60&sessionId=12&resId=0&materialId=paper&confId=189544.

[25] S. Fartoukh, "Breaching the Phase I optics limitations for the HL-LHC", Proceedings of Chamonix 2011 workshop on LHC Performance.

[26] S. Fartoukh, "Achromatic telescopic squeezing scheme and application to the LHC and its luminosity upgrade", Phys. Rev. ST Accel. Beams 16, 111002.

[27] S. Fartoukh et al, "The 10cm beta* MD", CERN-ATS-Note-2013-004 MD.

[28] R. De Maria, S. Fartoukh, A. Bogomyakov, M. Korostelev, "HLLHCV1.0: HL-LHC Layout and Optics Models for 150 mm Nb3Sn Triplets and Local Crab-cavities", IPAC 2013.

[29] R. Calaga et al, "Crab Cavity Workshop", Proceedings of Chamonix 2012 workshop on LHC Performance.

[30] E. Todesco, et al., (2013) Design studies of Nb3Sn quadrupole magnet for the high luminosity LHC. Submitted to: IEEE Trans. Appl. Supercond. *ASC Conference proceeding*, 2012 Portland.

[31] E. Todesco, et al. HiLumi PLC meeting, 26 March 2013.

[32] Q. Xu, et al., (2013) Design of a large single-aperture dipole magnet for HL LHC upgrade. Submitted to: IEEE Trans. Appl. Supercond. *ASC Conference proceeding*, 2012 Portland.

[33] S. Fartoukh, "Towards the LHC Upgrade using the LHC well characterized technology", sLHC-Project-report-0049, 2010.

[34] R. De Maria, S. Fartoukh, "Optics and Layout for the HL-LHC Upgrade Project with a Local Crab-Cavity Scheme," sLHC-Project-Report-55, 2011.

[35] S. Redaelli, Collimation Status and plans, 2nd joint HiLumi-Larp Annual meeting, Frascati, 2012, https://indico.cern.ch/contributionDisplay.py?contribId=61&sessionId=4&confId=183635.

[36] A. Ballarino, HiLumi WP6.

[37] J.-P. Koutchouk, "Principle of a correction of the long-range beam-beam effect in LHC using electromagnetic lenses", LHC Project Note 223, 2000, http://cds.cern.ch/record/692058.

[38] L. Esposito, F. Cerutti, "Energy deposition in the 150 mm baseline", WP3 meeting, 28 May 2013, https://lhc-div-mms.web.cern.ch/lhc-div-ms/tests/MAG/docum/hilumi/Presentations/2013-05-28_FLUKA_HL-LHC_EnDep.pptx.

[39] L. Esposito, F. Cerutti, "Update in energy deposition for the HL-LHC IR1-5", HiLumi WP2 Task leader meeting, 25th October, 2013, http://indico.cern.ch/materialDisplay.py?contribId=5&materialId=slides&confId=278765.

[40] S. Redaelli, Collimation Status and plans, 2nd joint HiLumi-Larp Annual meeting, Frascati, 2012,

https://indico.cern.ch/contributionDisplay.py?contribId=61&sessionId=4&confId=183635.

[41] G. Stancari, et al. "Beam halo dynamics and control with hollow electron beams", in Proceedings of the 52nd ICFA Advanced Beam Dynamics Workshop on High-Intensity and High-Brightness Hadron Beams (HB2012), http://arxiv.org/abs/1209.5380.

[42] R. Bruce, S. Redaelli, "Update on aperture margin estimation for HL-LHC", HiLumi WP2 Task Leader Meeting, 13 September 2013, http://indico.cern.ch/materialDisplay.py?contribId=1&materialId=slides&confId=270585.

[43] R. Bruce, "Apertures and protection for HL-LHC layouts (implication of tolerances and review of tolerances based on Run I experience) for different optics configurations (Round/Flat)", 3rd Joint HiLumi LHC-LARP Annual Meeting, https://indico.cern.ch/contributionDisplay.py?contribId=50&confId=257368.

[44] D. Banfi, J. Barranco, T. Pieloni, A. Valishev, "Required Beam-Beam separation for flat and round beams for 25 ns and considerations on the filling schemes", 19th HiLumi WP2 Task Leader Meeting, https://indico.cern.ch/getFile.py/access?contribId=0&resId=0&materialId=slides&confId=278323.

[45] D. Banfi, J. Barranco, T. Pieloni, A. Valishev, "Update on crossing angle scaling with bunch intensity", 20th HiLumi WP2 Task Leader Meeting, https://indico.cern.ch/getFile.py/access?contribId=6&resId=1&materialId=slides&confId=278765.

[46] R. Tomas, "IBS blow-up estimates and alternative scenarios for HL-LHC", 17th HiLumi WP2 Task Leader Meeting, https://indico.cern.ch/materialDisplay.py?contribId=3&materialId=slides&confId=272141.

[47] Input provided during the LIU Technical Meetings: http://indico.cern.ch/categoryDisplay.py?categId=4985.